TRENDS IN SCIENCES 2025; 22(10): 10421
https://doi.org/10.48048/tis.2025.10421 RESEARCH ARTICLE

Petrotectonics of Thoen Plutonic Rocks, Lampang Province, Eastern Granitic Belt of Thailand

Patcharin Kosuwan Jundee[1,*], Burapha Phajuy[1], Phisit Limtrakun[1], Apichet Boonsoong[1], Panjai Saraphanchotwitthaya[2], Ekkachak Chandon[3], Thanittha Suatrong[2] and Pinpan Thapthanee[1]

[1]Department of Geological Sciences, Faculty of Science, Chiang Mai University, Chiang Mai 50200, Thailand
[2]Department of Mineral Resources, Bangkok 10400, Thailand
[3]Science Laboratory for Education Division, Mahidol University, Kanchanaburi Campus, Kanchanaburi 71150, Thailand

([*]Corresponding author's e-mail: patcharinkosuwan.j@cmu.ac.th)

Received: 21 April 2025, Revised: 23 May 2025, Accepted: 9 June 2025, Published: 30 July 2025

Abstract

The plutonic rocks cropped in area of Thoen District, Lampang Province. The felsic to intermediate igneous rocks compositionally range from rhyolite, monzogranite to quartz monzonite, monzonite, granodiorite, diorite to gabbroic diorite with titanite as a minor constituent, characteristic of I-type granitic rocks. Based on minerals characters, 21 plutonic rock samples can be divided into 4 magmatic groups: Group I rhyolite, Group II monzogranite, Group III granodiorite and quartz monzonite, and Group IV granodiorite, diorite, monzonite and gabbroic diorite. Based on major and trace elements can be classified into 2 groups felsic to intermediate plutonic rocks and felsic volcanic rock (Group I, Group II and Group III) and intermediate mafic plutonic rocks (Group IV). The felsic intermediate plutonic rocks and felsic volcanic rock are the presence of mainly high-K calc-alkaline granite, I-type magma series that have active continental margins, with the involvement of continental crust. The intermediate to mafic plutonic rocks range from low-K to high-K calc-alkaline and shoshonitic series, indicating the feature of continental volcanic arc magma. All Thoen plutonic rocks have similar patterns in their chondrite and primitive mantle normalized patterns. Chondrite-normalized REE patterns are LREE enrichments and HREE depletion with negative Eu and Nb anomalies that are typical of volcanic arc granites. N-MORB normalized multi-element patterns are variable LILE enrichments (Rb, Ba, Th, Ce), HFSE depletions (Ta, Nb, Sr and Ti) and are typical of I-type volcanic arc granites. Thoen pluton is the part of EGB that indicates the magmatism along the boundary between Sukhothai Arc and Inthanon Zone.

Keywords: Thoen granite, I-type granite, Active continental margin, Post-collision, High-K calc alkalic rock, Eastern granitic belt

Introduction

The intrusive rocks in the SE Asia region have long been studied by many researchers and focused mainly on granitic rocks because they are voluminous, and are related to economic minerals such as tin-tungsten, precious metals, and rare earth elements (REE) minerals [1-6]. The granitic rocks in Thailand and SE Asia are separated into 3 granitic belts: Western (WGB), central main range (CGB), and eastern (EGB), based on their distribution and geochemistry as illustrated in **Figure 1(a)**. Each granitic belt in Thailand are difference in occurrence, tectonic setting and economic minerals relationship. A clear and precise division of granitic zone can facilitate the future utilization. The rock forming minerals and geochemical character of granitic rocks can be indicator for tectonic setting and granitic zone dividing. The plutonic rocks in

Thoen district, Lampang Province are scattering crop out as small plutons in alluvial sedimentary deposit along the western part of the Wang River. Based on the location of the Thoen plutonic outcrop and some previous works, it is uncertain whether the Thoen plutonic is part of the CGB or EGB. This study aimed to petrochemically characterize the plutonic rocks in Thoen area that provide information on tectonic environments of formation. This information provides some clues for interpreting the tectonic evolution of Thailand and divides granitic zone.

Geological background

The western granitic belt (WGB) extends along the Thai-Myanmar border, Phuket Island (Thailand), and Aceh and Sumatra islands (Indonesia). The WGB whole-rock geochemistry is granite, granodiorite and monzodiorite, and has high-K calc-alkaline, peraluminous and S-type signatures. The central main range granitic belt (CGB) is the main granitoid in Thailand and SE Asia, and occurs as plutons with continuous north-south orientation, in northern-central and southern Thailand, the main range of Malaysia, and the Bangka, Singkep, and Tuju Islands of Indonesia [2,7]. The CGB in northern Thailand can be divided into 2 sub-belts including western and eastern sub-belts. The western sub-belt is situated in the southern part of Mae Hong Son Province along the Thai-Myanmar border and consists largely of composite plutons (Mae Sariang complex) extending from Pai District [8] through Samoeng, Mae Chaem, and Hot Districts and Doi Inthanon Mountains, Chiang Mai Province, to the western part of Tak Province. The eastern sub-belt comprises the Mae Chan pluton in Chiang Rai Province, the Fang-Mae Suai-Wiang Pa Pao batholith [9] in Chiang Mai Province and the Khuntan batholith in Lamphun Province to the western part of Tak Province. In the southern part of the Mae Ping fault [10], the CGB is distributed from western Thailand to southern Thailand. The CGB rocks are granite, granodiorite and monzodiorite, and have high-K calc-alkaline, peraluminous and S-type signatures. The tectonic settings of formation were syn-collision and post-collision [7-12]. Their absolute ages in northern Thailand, determined by $^{40}Ar/^{39}Ar$ dating, are 220 - 180 Ma (Late Triassic - Middle Jurassic) [2] and the zircon U-Pb ages of granite in the Mae Suai area, Chiang Rai Province is 220 + 1 (Late Triassic) [13,14]. The eastern granitic belt (EGB) is distributed along the Korat Plateau edge in central to eastern Thailand and is related to metal minerals such as ilmenite and magnetite. The EGB rocks are granite, granodiorite and monzodiorite; their whole-rock geochemistry is calc-alkaline, metaluminous, and I- to A-type. Zircon U-Pb dating of granite yields ages of 208 - 226 Ma (Late Triassic), corresponding to the collision of Sibumasu and Indochina terranes and some dates to 55 Ma (Eocene) are likely related to the collision of Indian and Eurasian continents [15-18].

Geological data of Lom Rat sub-district, Thoen District, Lampang Province, compiled by Piyasin [19] and Department of Mineral Resources (DMR) [20], reported the Permian sedimentary and volcano-sedimentary rocks (Png1), Permo-Triassic volcanic rocks (PTrv), Triassic sedimentary rocks (Trpt), Triassic granite (Trgr), Quaternary terrace sediments (Qt) and Quaternary alluvial sediments (Qa) (**Figure 1(b)**). Permian sedimentary and volcano-sedimentary rocks (Png1) are tuffaceous sandstone, sandstone, greenish-gray shale, and limestone. Permo-Triassic volcanic rocks (PTrv) are rhyolite, andesite, welded tuff, volcanic breccia, rhyolitic tuff, and andesitic tuff. Triassic sedimentary rocks (Trpt) are sandstone, siltstone, and red conglomerate. Quaternary terrace sediments (Qt) are gravel, sand, silt, clay, and laterite. Quaternary alluvial sediments (Qa) are sediments such as gravel, sand, silt, and clay. The igneous rocks in these studies are Triassic granite (Trgr) composed of biotite granite, tourmaline granite, granodiorite, biotite-muscovite granite, muscovite-tourmaline granite, biotite-tourmaline granite and biotite-hornblende granite; porphyritic granite, pinkish granite including quartz veins.

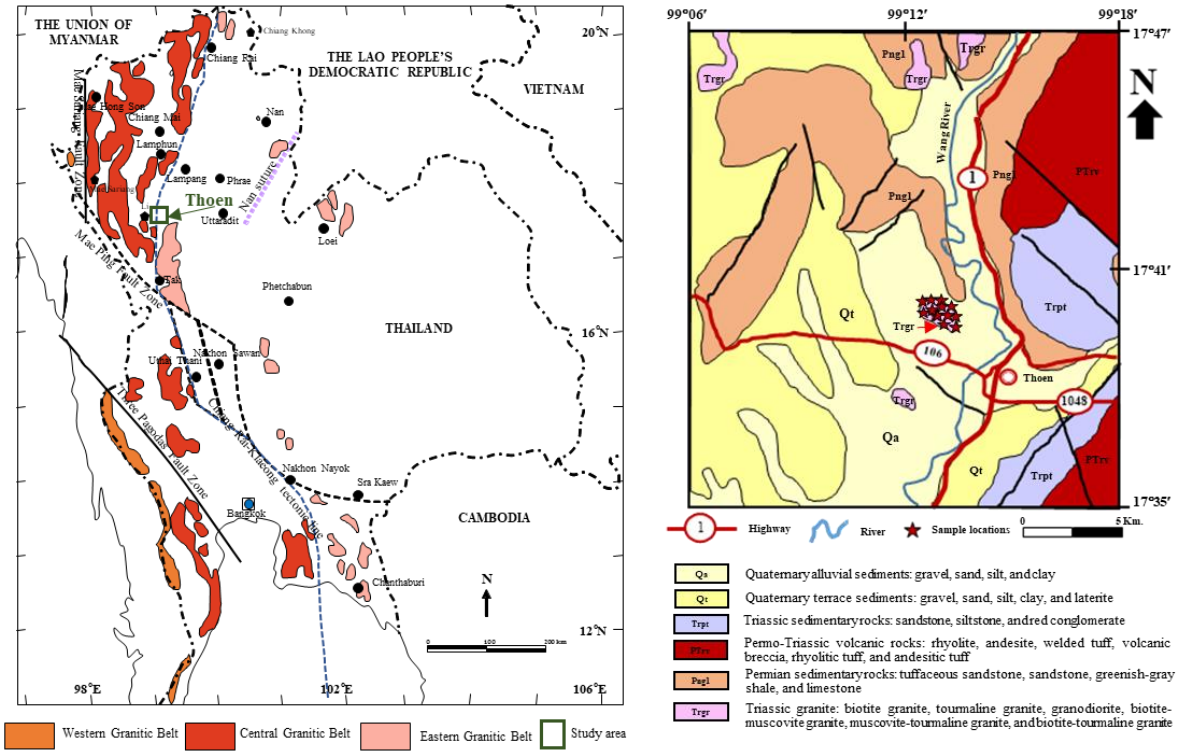

Figure 1 (a) Map showing the distribution of western, central main range and eastern granitic belts in Thailand, and tectonic line boundaries, modified from Moley [10], Xin *et al.* [14], Jundee *et al.* [8] and Jundee *et al.* [9], and study location, and (b) geological map of the study area, modified from Piyasin **[**19**]** and DMR [20].

Materials and methods

Sample collection and selection

Twenty-one igneous rock samples were carefully selected to obtain least-altered samples from outcrops. The samples were generally mesoscopic domains selected without secondary minerals, such as quartz resulting from silicification, epidote minerals and chlorite, displaying well-developed foliation or mineral layering samples, and abundant vugs or druses, xenocrysts, and xenoliths, quartz, epidote, or calcite veining/ patches totalling more than 5 modals%.

Sample preparation

The rock samples were prepared as standard thin sections, rock slabs, and sample powder. The felsic rock slabs were stained to differentiate K-feldspar from plagioclase using amaranth and sodium cobaltinitrite solutions [21]. Modal analysis based on 400 counts was done on stained medium-grained, felsic rock slabs, unstained medium-grained, mafic rock slabs and thin sections and fine-grained felsic rocks was performed under a petrographic microscope. The samples were crushed into small chips by using a Rocklabs Hydraulic Splitter/Crusher. Approximately 50 - 80 g sample chips were cautiously chosen, cleaned and pulverized for a few minutes by a Rocklabs Tungsten-Carbide Ring Mill.

Analytical techniques

The sample powders were chemically analyzed for major oxides, trace elements, rare-earth elements (REEs), and loss on ignition (LOI). Rock-powdered samples were prepared as fused glass beads and pellets. Chemical analyses of major and minor oxides (SiO_2, TiO_2, Al_2O_3, total iron (FeO and Fe_2O_3) as Fe_2O_3, MnO, MgO, CaO, Na_2O, K_2O and P_2O_5) and some certain trace elements (Ba, Rb, Sr, Y, Zr, Nb, Ni, V, Sc, Cr and Th) were carried out using a PANalytical Zetium X-ray fluorescence (XRF) spectrometer (wavelength dispersive system), installed at the Geoscience program, Kanchanaburi campus, Mahidol University, Thailand. The standards used were the set of SARM standards (GS-N, MA-N, BE-N) [22] and GSJ Igneous standards (JG-2, JB-2a, JB-3) [23] with Ausmon111 Drift Monitor. These major elements were measured from fused glass beads that prepared with 0.5 g powdered sample and 6.5 g mixer materials (anhydrous lithium

tetraborate ($Li_2B_4O_7$) 49.75%, lithium metaborate ($LiBO_2$) 49.75% and lithium bromide (LiBr) 0.5%) and from pressed powders prepared with 4 g sample powder and 1 g XRF binder (Licowax) for trace elements. Detection limits for Ba are 50 ppm, whereas Rb, Sr, Ni, V, Cr and Zr are 10 ppm, and Y, Nb, Sc and Th are 5 ppm. Ignition loss was done by heating approximately 1 g of powdered samples at 900 °C for 1 h. Some certain trace elements (Th and U) and REEs (La, Ce, Pr, Nd, Sm, Eu, Gd, Tb, Dy, Ho, Er, Tm, Yb and Lu) were determined on all the samples, using a PerkinElmer's NexION® 2000 Inductively Coupled Plasma Mass Spectrometer (ICP-MS). Solutions for ICP-MS analysis were prepared using the microwave digestion technique. The standards used in the ICP-MS analysis were the international standard JA-1 and JB-1a. These procedures were done at DMR.

Results and discussion

Field occurrence and petrography

The igneous rocks are cropped out in the Lom Rat subdistrict area, Thoen District, Lampang Province. The igneous rocks in the study area appear as small outcrops and are not recorded on existing geological maps, which are difficult to observe because they are covered by alluvial sediments. They are composed mainly of granitic rocks and intermediate rocks with minor rhyolitic rock. All the samples are collected from out croup.

Group I rhyolite have 2 samples (sample TH14 and TH20). The rock samples are fine-grained and commonly show a moderately porphyritic texture (**Figure 2**). The essential minerals found are quartz (39 - 41 modal%), K-feldspar (27 - 28 modal%), plagioclase (24 - 25 modal%), and accessory minerals including biotite (4 - 7 modal%), muscovite (0.5 - 1 modal%), primary titanite (1 modal%) and zircon (1 - 2 modal%). Quartz phenocrysts are anhedral to euhedral outlines with sizes ranging from 0.5 to 1.1 mm across. K-feldspar phenocrysts are subhedral with sizes ranging from 0.4 to 1.2 mm across, and groundmass of anhedral K-feldspar. K-feldspar are slightly altered to clay minerals. Plagioclase phenocrysts have sizes ranging from 0.3 to 3.0 mm across. Subhedral-euhedral outlines plagioclase phenocrysts and anhedral groundmass are slightly altered to sericite and chlorite. Biotite and muscovite are subhedral outlines. Biotite exhibits yellowish-brown to dark brown pleochroism, slightly altered to sericite, chlorite, titanite/leucoxene and epidote. Zircon shows subhedral to euhedral outlines and is inclusions in biotite. Primary titanite shows a subhedral outline.

Group II rocks (sample TH02, TH08, TH092, TH13, TH15, TH16 and TH17) are all monzogranite (**Figure 2**). They are coarse-grained and seriate-textured or non-porphyritic textures, consisting essentially of K-feldspar (13 - 37 modal%), quartz (19 - 35 modal%) and plagioclase (23 - 30 modal%), with common accessory biotite (0 - 12 modal%), muscovite (2 - 24 modal%), opaque mineral (0 - 2 modal%), primary titanite (0 - 3 modal%), epidote, and zircon (0 - 1 modal%). K-feldspar is anhedral-euhedral outlines. Quartz is an anhedral outline. Plagioclase has a subhedral outline and is slightly altered to sericite and clay minerals. Biotite and muscovite have subhedral outlines. The biotite exhibits yellowish-brown to dark brown pleochroism and is slightly altered to chlorite. Zircon shows subhedral to euhedral outlines and is biotite inclusions. Opaque minerals show anhedral to subhedral outlines and are slightly altered to titanite and Fe-Ti oxide minerals. Primary titanite show euhedral and subhedral outlines with size up to 0.2 mm across. Hornblende is subhedral and generally displays yellow to pale green pleochroism in samples TH13, TH15 and TH17.

Group III includes granodiorite (sample TH03 and TH18) and quartz monzonite (sample TH122). These rock samples are coarse-grained, with seriate or non-porphyritic textures (**Figure 2**). The major mineral compositions are plagioclase (27 - 34 modal%), K-feldspar (21 - 34 modal%), quartz (12 - 14 modal%), hornblende (16 - 19 modal%), while minor mineral compositions are biotite (5 - 15 modal%), muscovite (0 - 1 modal%), zircon (0 - 2 modal%), and small amounts of primary titanite and opaque mineral (0 - 3 modal%). The plagioclase shows anhedral to subhedral outlines and is slightly altered to sericite, chlorite and clay minerals. K-feldspar is subhedral and slightly altered to clay minerals. Quartz is anhedral and interstitial to other minerals. Hornblende shows anhedral to euhedral outlines, has dark green to pale green pleochroism and is slightly altered to chlorite, titanite, and opaque minerals. Biotite and muscovite have subhedral outlines. The biotite exhibits pale to dark greenish-brown pleochroism and is slightly altered to sericite, chlorite, titanite/leucoxene, epidote and opaque minerals. Zircon

shows subhedral to euhedral outlines. Primary titanite shows a subhedral outline with a size up to 0.25 mm across. Opaque minerals shows anhedral to subhedral outlines and are moderately altered to titanite and Fe-Ti oxide minerals.

Group IV is mainly diorite (sample TH04, TH05, TH10 and TH121) and monzonite (sample TH01, TH11), with minor of granodiorite (sample TH06) and gabbroic diorite (sample TH07). These rock samples are coarse-grained, with seriate or non-porphyritic texture (**Figure 2**). Their major constituents are plagioclase (21 - 46 modal%), hornblende (5 - 43 modal%), K-feldspar (6 - 28 modal%), and quartz (5 - 18 modal%), while minor constituents are biotite (0 - 17 modal%), and muscovite (0 - 18 modal%), and small amounts of zircon (0 - 2 modal%), primary titanite (0 - 2 modal%) and opaque minerals (0 - 2 modal%). The plagioclase shows subhedral to subhedral outlines with a lathed shape and is slightly altered to sericite, chlorite and clay minerals. Hornblende shows anhedral to euhedral outlines and has yellowish-green to dark green pleochroism and is slightly altered to chlorite, titanite, and opaque minerals. K-feldspar is subhedral, and slightly altered to clay minerals. Quartz is anhedral to subhedral outlines and interstitial to other minerals. Biotite and muscovite have subhedral outlines. The biotite exhibits pale to dark greenish brown pleochroism and is slightly altered to sericite, chlorite, titanite, epidote and opaque minerals. Zircon shows a subhedral outline. Primary titanite show subhedral to euhedral outlines with size up to 0.3 mm across. Opaque minerals show anhedral to subhedral outlines and are slightly altered to titanite/leucoxene and Fe-Ti oxide minerals.

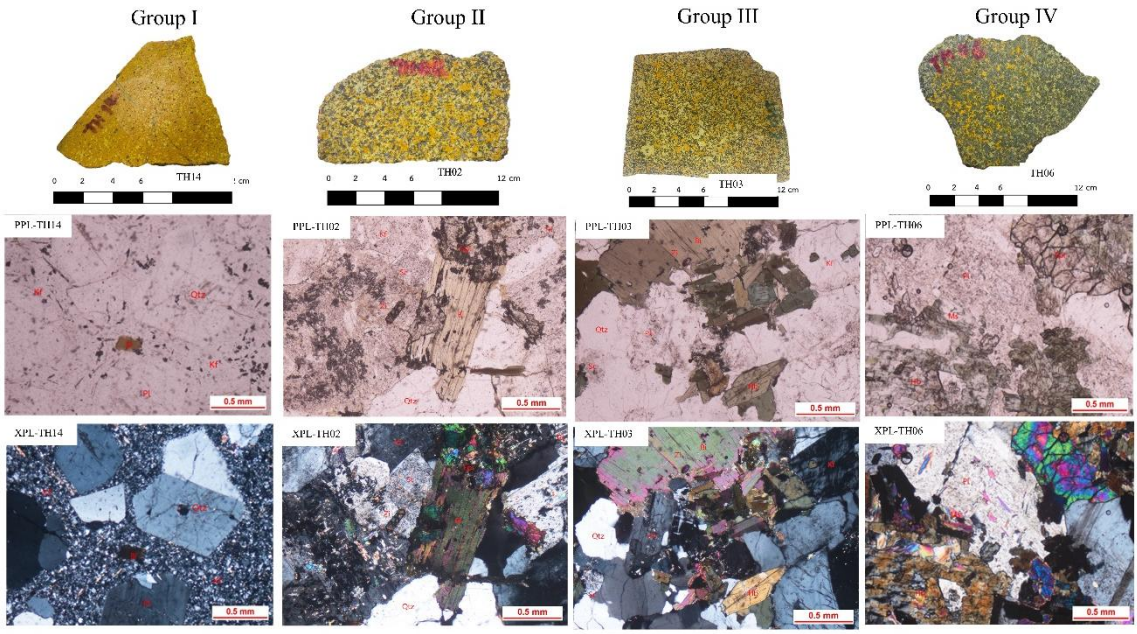

Qtz=quartz, Pl=plagioclase, Kf =alkaline feldspar, Bi=biotite, Ms=Muscovite, Zr=zircon, Epi= epidote, Hb=hornblende
PPL = plane polarized light, XPL = cross polarized light

Figure 2 The petrography of representative rock sample groups.

Geochemical characteristics

The rock samples were divided into 4 groups (**Table 1**) based on the texture of the rock and the REE pattern. Almost all the studied, plutonic samples (Group II, Group III, and Group IV) are medium to coarse-grained, except for Group I (sample nos. TH14 and TH20), which is fine-grained and have modal mafic minerals less than 90 %. They have been classified based on their modal quartz, alkali feldspar, and plagioclase composition according to the QAP modal classification of plutonic rocks (**Figure 3(a)**) [24]. The QAP diagram of plutonic rocks shows that the studied samples are monzogranite, quartz monzonite, quartz monzodiorite and granodiorite. Sample nos. TH14 and TH20 (Group I) are felsic volcanic rocks that fall within the monzogranite field of the QAP diagram of plutonic rocks.

Table 1 Modal analyses of the studied plutonic rocks in terms of volume%.

Group	Group I Rhyolite		Group II Monzogranite						
Sample number	**TH14**	**TH20**	**TH02**	**TH08**	**TH092**	**TH13**	**TH15**	**TH16**	**TH17**
Quartz	40.25	39.25	23.75	23.50	25.75	25.75	19.75	34.25	23.00
K-Feldspar	28.00	27.75	36.00	36.25	35.75	13.75	35.50	31.25	28.75
Plagioclase	24.00	24.25	27.75	26.25	29.75	25.75	28.00	23.75	24.75
Hornblende	nd	nd	nd	nd	nd	10.00	1.00	nd	nd
Biotite	4.50	6.25	8.50	9.75	4.50	nd	9.00	4.75	11.50
Muscovite	1.00	0.50	2.00	3.25	3.00	23.50	5.00	4.50	5.25
Opaque mineral	nd	nd	1.25	0.75	1.25	1.25	1.25	1.25	3.50
Titanite	1.00	1.00	tr	tr	tr	tr	tr	tr	2.50
Zircon	1.25	1.00	0.75	0.25	nd	nd	0.50	0.25	0.75
sum	100	100	100	100	100	100	100	100	100

Group	Group III Granodiorite and quartz monzonite			Group IV Diorite, monzonite, granodiorite and gabbroic diorite								
Sample number	**TH03**	**TH122**	**TH18**	**TH01**	**TH04**	**TH05**	**TH06**	**TH07**	**TH091**	**TH10**	**TH11**	**TH121**
Quartz	13.50	13.00	12.75	10.75	8.75	12.50	5.00	12.50	17.50	10.00	10.00	8.50
K-Feldspar	25.00	33.50	21.25	15.50	28.00	12.25	6.75	35.00	11.25	13.50	18.75	14.00
Plagioclase	33.75	27.00	29.75	29.75	26.75	32.00	27.00	27.50	46.00	35.25	21.75	33.25
Hornblende	18.50	16.50	18.25	26.75	22.00	31.25	42.00	5.00	23.50	25.50	37.50	29.75
Biotite	8.00	5.00	15.00	16.00	13.25	10.50	nd	16.25	nd	13.25	10.75	11.25
Muscovite	1.00	nd	nd	nd	nd	0.75	17.75	2.50	0.75	nd	nd	nd
Opaque mineral	tr	3.00	1.75	nd	0.75	0.50	1.00	0.50	0.75	1.75	1.25	2.00
Titanite	tr	2.00	tr	md	tr	tr	tr	nd	tr	nd	tr	tr
Zircon	0.25	nd	1.25	1.25	0.50	0.25	0.50	0.75	0.25	0.75	tr	1.25
sum	100	100	100	100	100	100	100	100	100	100	100	100

tr = trace, nd = not detected

The chemical concentrations of the rocks are given in **Table 2**. The alteration box plot of Large *et al.* [25] has been applied to the studied samples to test their nature. The major oxides (weight%) were calculated following the Ishikawa alteration index (AI) and chlorite-carbonate-pyrite index (CCPI) equations.

$$AI = \frac{100(MgO + K_2O)}{(FeO + K_2O + MgO + Na_2O)}$$

$$CCPI = \frac{100(FeO + MgO)}{(FeO + K_2O + MgO + Na_2O)}$$

The alteration box plot (**Figure 3(b)**) show that the studied samples lie almost totally in the field of felsic to mafic rocks and confirms the nature of the carefully selected samples, except 3 samples are outside the field but very close to the field boundary of felsic rocks.

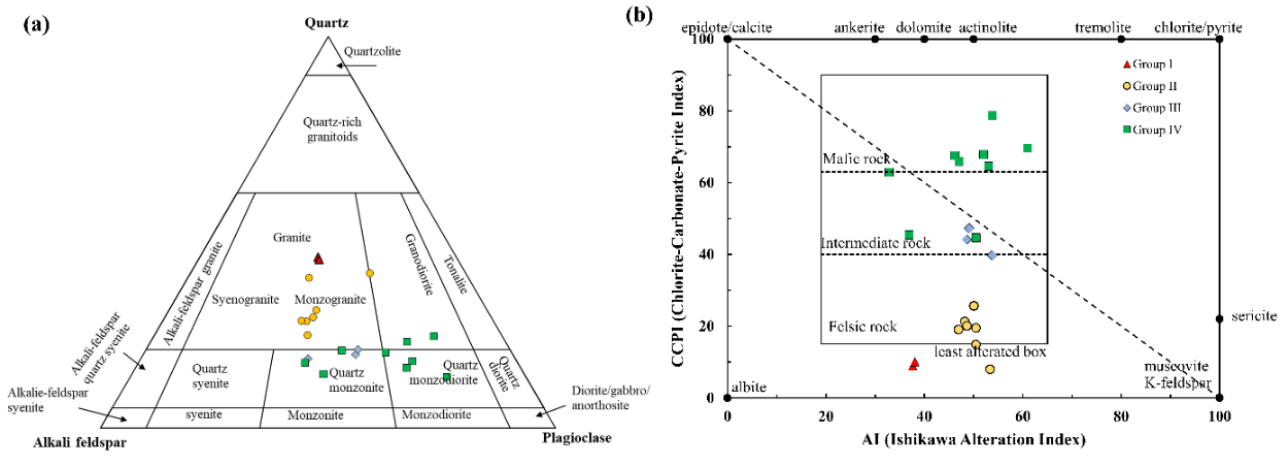

Figure 3 (a) IUGS classification of plutonic rocks with mafic minerals less than 90 modal% [24] showing positions of the studied plutonic rocks and (b) alteration box plot [25] of the studied plutonic rocks.

Table 2 Major and minor oxides, certain trace elements, and REE of the studied plutonic rocks.

Rock Group	Group I Rhyolite		Group II Monzogranite						
Samples	**TH14**	**TH20**	**TH02**	**TH08**	**TH092**	**TH13**	**TH15**	**TH16**	**TH17**
Major and minor oxides (wt%)									
SiO_2	74.20	74.07	72.02	72.68	75.86	74.98	73.28	71.81	71.96
TiO_2	0.06	0.07	0.21	0.19	0.05	0.18	0.18	0.18	0.28
Al_2O_3	15.15	15.23	15.34	14.90	14.12	14.28	14.68	15.17	14.90
Fe_2O_3*	0.60	0.67	1.57	1.43	0.53	1.06	1.38	1.54	1.92
MnO	0.02	0.02	0.04	0.03	0.01	0.02	0.03	0.04	0.04
MgO	0.21	0.25	0.59	0.54	0.16	0.35	0.54	0.29	0.73
CaO	1.40	1.43	2.20	2.27	1.28	1.07	1.95	3.15	2.40
Na_2O	5.10	5.01	3.68	3.63	3.52	3.62	3.49	3.56	3.24
K_2O	3.23	3.24	4.30	4.26	4.47	4.41	4.42	4.21	4.44
P_2O_5	0.02	0.02	0.06	0.05	0.00	0.03	0.05	0.05	0.08
LOI	0.44	0.58	0.96	0.90	0.86	0.88	0.76	0.72	0.78
Total	99.03	99.18	98.32	99.89	99.96	99.60	99.89	99.38	99.30
Trace elements (ppm)									
Ba	1,851	1858	957	869	769	1225	904	850	961
Rb	144	140	250	269	219	221	249	255	253
Sr	1,430	1438	393	383	350	290	365	456	334
Y	27	27	41	41	35	35	40	39	43
Zr	132	136	141	129	98	142	126	121	157
Nb	16	19	21	19	25	22	19	17	20
Ni	19	20	34	19	22	27	36	30	33
Cr	9	16	32	193	9	161	69	75	108
V	6	8	16	17	1	18	15	12	23
Sc	1	4	7	7	4	11	5	4	6
Th	11	13	23	22	19	31	23	24	35
Ti	383	432	1262	1156	302	1075	1082	1051	1703
P	75	71	282	238	13	133	225	203	368
Rare earth elements (ppm)									
La	5	12.2	32.5	23.2	8.7	13.9	26.7	18.4	49
Ce	7.4	22.6	65.3	46.2	19.4	24.1	39.8	37.9	69.4
Pr	1.3	3.12	7.43	5.05	2.4	3.43	5.25	4.09	10.09
Nd	4.8	11.4	26.2	17.7	8.9	12.2	18.3	14.2	35.4
Sm	0.94	1.93	4.31	2.92	1.82	2.16	2.99	2.38	5.44
Eu	0.32	0.44	0.78	0.54	0.49	0.44	0.58	0.47	0.93
Gd	0.86	1.46	3.19	2.24	1.63	1.62	2.37	1.79	3.96
Tb	0.13	0.19	0.4	0.28	0.26	0.21	0.3	0.22	0.48
Dy	0.88	1.07	2.07	1.45	1.6	1.13	1.58	1.22	2.55
Ho	0.18	0.21	0.37	0.26	0.31	0.2	0.29	0.22	0.46
Er	0.57	0.63	1.02	0.73	0.9	0.6	0.8	0.63	1.29
Tm	0.09	0.1	0.14	0.1	0.14	0.09	0.11	0.09	0.18
Yb	0.66	0.71	0.94	0.69	0.95	0.61	0.74	0.59	1.13
Lu	0.11	0.11	0.15	0.11	0.15	0.1	0.13	0.09	0.18

Rock Group	Group III Granodiorite and quartz monzonite			Group IV Diorite, monzonite, granodiorite and gabbroic diorite								
Samples	**TH03**	**TH122**	**TH18**	**TH01**	**TH04**	**TH05**	**TH06**	**TH07**	**TH091**	**TH10**	**TH11**	**TH121**
Major and minor oxides (wt%)												
SiO_2	66.82	66.33	65.78	58.19	59.48	61.58	66.97	52.42	65.05	58.51	57.68	59.45
TiO_2	0.45	0.46	0.51	0.60	0.67	0.44	0.46	0.83	0.45	0.66	0.57	0.68
$Al2O_3$	15.59	14.82	15.91	14.72	15.49	16.24	15.62	13.34	17.11	15.37	13.13	14.43
Fe_2O_3*	3.67	3.27	3.75	5.82	6.89	5.27	3.68	8.09	2.89	6.54	6.34	6.40
MnO	0.07	0.06	0.06	0.15	0.12	0.12	0.06	0.15	0.06	0.12	0.12	0.12
MgO	2.25	2.14	2.59	6.47	5.13	3.77	2.29	9.69	2.05	5.21	8.62	6.32
CaO	3.51	4.56	4.16	7.07	6.23	7.12	3.35	10.33	6.31	7.19	6.80	6.35
Na_2O	3.22	3.03	3.08	3.10	2.69	4.39	2.95	2.34	3.97	2.90	2.04	2.60
K_2O	4.27	5.18	3.99	3.64	3.09	0.96	4.47	2.47	1.97	3.18	4.50	3.44
P_2O_5	0.16	0.15	0.18	0.23	0.21	0.12	0.16	0.34	0.15	0.31	0.19	0.20
LOI	0.94	0.68	0.90	0.70	1.72	0.58	1.36	1.52	1.04	1.30	0.74	1.06
Total	98.69	98.17	98.71	102.89	98.17	97.62	99.36	97.85	98.84	98.10	97.90	98.00
Trace elements (ppm)												
Ba	936	1,407	1,489	1,002	874	214	926	1,089	596	1,224	1,819	1,028
Rb	211	144	147	152	116	38	79	185	52	111	113	134
Sr	362	380	583	333	315	230	503	407	523	514	380	325
Y	40	36	32	23	34	24	26	36	25	32	30	35
Zr	167	169	175	146	138	73	144	168	183	140	145	101
Nb	15	23	13	8	14	18	15	15	17	15	16	20
Ni	65	60	73	143	139	23	272	75	60	98	295	176
Cr	157	65	198	368	242	148	653	209	79	283	691	398
V	43	34	49	56	64	33	59	46	32	64	56	69
Sc	13	4	11	18	19	15	22	13	6	23	16	19
Th	25	26	20	22	18	9	18	18	38	21	20	14
Ti	2,692	2,736	3,051	3,601	4,008	2,625	2,758	4,984	2,678	3,962	3417	4,068
P	683	672	781	1012	928	522	699	1491	638	1343	844	873
Rare earth elements (ppm)												
La	51.2	28.7	58.3	30.5	39	19.6	52.5	44	36.4	45	22.4	20
Ce	102.2	83.2	124.2	66.7	77	40.5	108	75	72.6	112.4	65	53.4
Pr	11.11	8.92	12.16	8.67	8.93	6.2	14.37	9.49	9.96	12.81	8.83	8.3
Nd	39.7	36	41.6	33.7	33.3	25.7	56.4	34.6	36.9	51.2	37.1	37.3
Sm	6.93	7.89	6.11	6.39	6.1	5.36	9.81	6.13	6.6	9.47	7.07	8.16
Eu	1.32	1.42	1.32	1.35	1.35	1.45	1.95	1.23	1.31	1.82	1.59	1.58
Gd	5.39	6.34	4.46	5.19	5.92	4.64	7.25	4.81	5.01	7.19	5.41	6.49
Tb	0.7	0.88	0.52	0.71	0.86	0.67	0.89	0.63	0.66	0.92	0.69	0.9
Dy	3.78	4.97	2.69	4.01	4.95	4.06	4.56	3.39	3.65	4.91	3.79	5.05
Ho	0.7	0.94	0.49	0.76	0.95	0.81	0.8	0.63	0.69	0.9	0.69	0.94
Er	1.96	2.59	1.3	2.2	2.6	2.38	2.05	1.76	1.93	2.42	1.91	2.63
Tm	0.27	0.36	0.18	0.31	0.34	0.34	0.27	0.24	0.27	0.32	0.27	0.35
Yb	1.69	2.23	1.05	2.02	2.15	2.24	1.61	1.5	1.74	1.96	1.7	2.19
Lu	0.26	0.32	0.17	0.32	0.34	0.36	0.25	0.23	0.27	0.3	0.26	0.33

Magmatic grouping has been carried out, based on occurrences, petrography and geochemistry, particularly chondrite-normalized REE and N-MORB normalized multi-element patterns. The presented can be divided into 4 magmatic groups as Group I rhyolite (monzogranite), Group II monzogranite, Group III quartz monzonite and granodiorite, and Group IV monzonite, granodiorite, diorite and gabbroic diorite. The studied plutonic samples have a wide range of compositions that are acid to base with 52.45 - 75.86 wt% SiO_2. The geochemical compositions seem to form a board, continuous fractionation trends on $Na_2O + K_2O$ versus SiO_2 (**Figure 4(a)**) [26,27], AFM (**Figure 4(b)**) [28] plots, and K_2O versus SiO_2 plot (**Figure 4(c)**) [29] suggestive of co-magmatic origin. The chondrite-normalizing rare earth elements (REE) pattern is used for considerable tectonic settings. The chondrite-normalizing values used are those of Taylor and Gorton [30]. The REE are the incompatible elements in igneous rock with atomic numbers 57 - 71 (La-Lu) that have

similar geochemical behavior [31]. The MORB (N-MORB) normalized multi-element diagram is used N-MORB normalized values from Sun and McDonough [32] that represented the large-ion lithophile elements (LILE), e.g. Cs, Rb, K, Ba, Sr and Eu, and high-field strength elements (HFSE), e.g. Y, Hf, Zr, Ti, Nb and Ta. The chondrite-normalized REE patterns (**Figure 5(a)**) and N-MORB normalized patterns (**Figure 5(b)**) of the rock samples seem to parallel trends that support the co-magmatic origin [31].

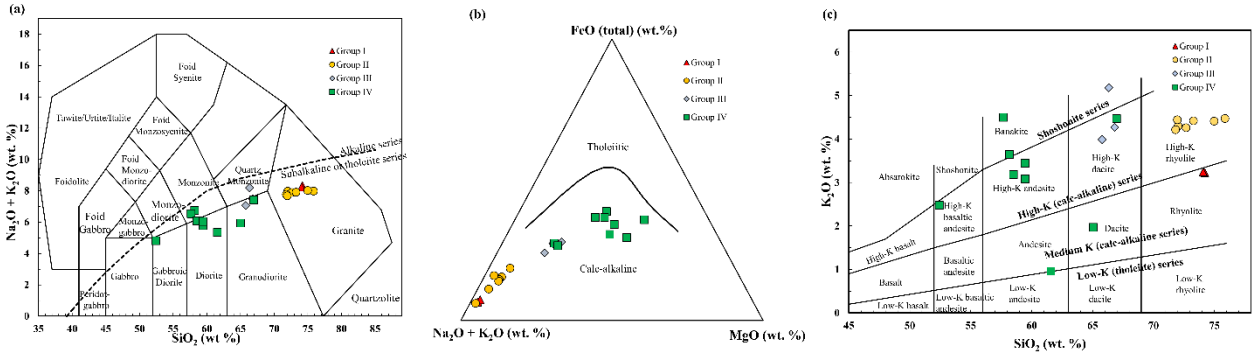

Figure 4 Positions of the studied plutonic rocks in the TAS diagram [26] with the tholeiitic - calc-alkaline boundary line of Irvine and Baragar [27], AFM diagram [28] and (c) K_2O versus SiO_2 diagram [29].

Group I rocks are monzogranite, sub-alkaline or tholeiitic series on total alkalis - SiO_2 (**Figure 4(a)**) [26,27]. These rocks are the calc-alkaline in the field of AFM plot (**Figure 4(b)**) [28] and medium-K, calc-alkaline signatures on the K_2O versus SiO_2 plot (**Figure 4(c)**) [29]. The medium-K, calc-alkaline series of Group I rocks is strongly supported by their chondrite-normalized REE patterns [30] that have relatively flat heavy REE (HREE) from Yb to Dy, and light REE (LREE) enrichment from Dy to La (**Figure 5(a)**). The values for chondrite normalized Dy/Yb ((Dy/Yb)cn) and La/Dy ((La/Dy)cn) are 0.85 - 0.96 and 5.86 - 11.76, respectively and show slightly positive Eu. The N-MORB normalized multi-element patterns [32] do not show negative Nb anomaly (**Figure 5(b)**).

Group II rocks are granite, sub-alkaline or tholeiitic series on total alkalis - SiO_2 (**Figure 4(a)**) [26,27]. These rocks form a linear fractionation trend, caused by the removal of Fe-Mg minerals, in the calc-alkaline field of the AFM plot (**Figure 4(b)**) [28] and have high-K, calc-alkaline signatures on the K_2O versus SiO_2 plot (**Figure 4(c)**) [29]. The high-K calc-alkaline series of Group II rocks are strongly supported by their chondrite-normalized REE patterns [30] that have relatively flat heavy REE (HREE) from Yb to Dy, and light REE (LREE) enrichment from Dy to La (**Figure 5(a)**). The values for chondrite normalized Dy/Yb ((Dy/Yb)cn) and La/Dy ((La/Dy)cn) are 1.08 - 1.44 and 5.61 - 19.83, respectively and show negative Eu. The N-MORB normalized multi-element patterns [32] do not show negative Nb anomaly (**Figure 5(b)**).

Group III rocks are sub-alkaline or tholeiitic rocks on total alkalis - SiO_2 (**Figure 4(a)**) [26,27]. The rocks are calc-alkaline on the AFM plot (**Figure 4(b)**) [28] and high-K calc-alkaline to shoshonitic series on the SiO_2 versus K_2O plot (**Figure 4(c)**) [29]. The high-K calc-alkaline series of Group III rocks are strongly supported by their chondrite-normalized REE patterns [30] that have relatively flat heavy REE (HREE) from Yb to Dy, and light REE (LREE) enrichment from Dy to La (**Figure 5(a)**). The values for chondrite normalized Dy/Yb ((Dy/Yb)cn) and La/Dy ((La/Dy)cn) are 1.43 - 1.64 and 5.96 - 22.36, respectively and show negative Eu. The N-MORB normalized multi-element patterns [32] do not show negative Nb anomaly (**Figure 5(b)**).

Group IV rock is intermediate to mafic rocks that have SiO_2 of about 52 - 61 wt%. It is sub-alkaline or tholeiitic rocks on total alkalis - SiO_2 (**Figure 4(a)**) [26,27]. The rocks are calc-alkaline on the AFM plot (**Figure 4(b)**) [28] and appear to range from low K to high-K calc-alkaline and shoshonitic series on the SiO_2 versus K_2O plot (**Figure 4(c)**) [29]. The transitional shoshonitic to high-K calc-alkaline affinity is strongly supported by its chondrite-normalized REE pattern [30] (**Figure 5(a)**). The pattern shows relatively flat HREE from Yb to Dy ((Dy/Yb)cn = 1.27 – 1.81) and light REE

enrichment from Dy to La ((La/Dy)cn = 4.09 – 13.39), similar to the patterns of Group III. The REE patterns show negative Eu. The N-MORB normalized multi-element patterns [32] show negative Nb anomaly (**Figure 5(b)**).

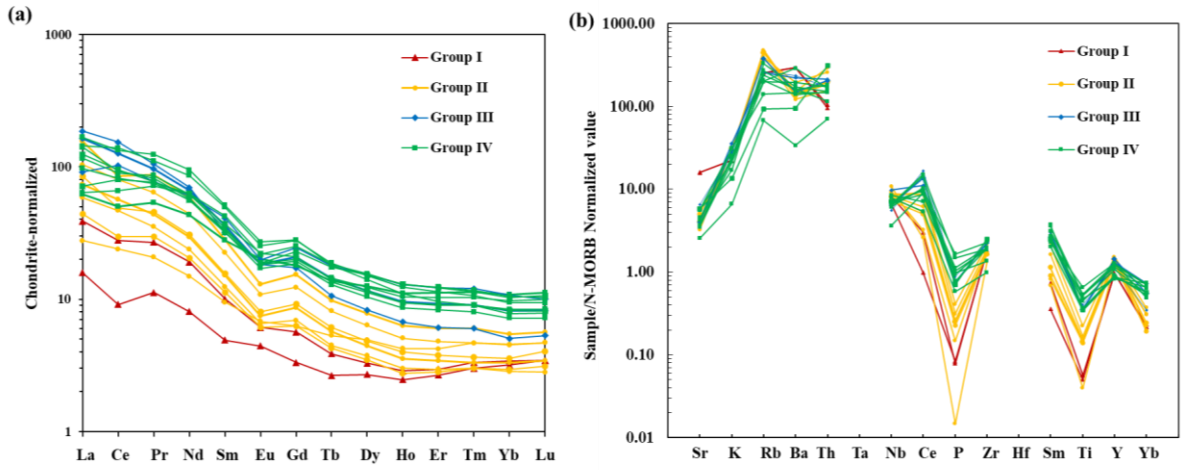

Figure 5 (a) chondrite-normalized REE patterns [30] and (b) N-MORB normalized multi-element patterns [32] of the plutonic rocks.

Tectonic setting

Some certain elements incompatible and compatible with typical mantle mineralogy were used as normalized multi-element diagrams that are a useful power tool in determining tectonic setting of formation. The order of element incompatibility may change significantly in different tectonic environments, physical conditions and mineral assemblages. The LILE concentrations may be a function of the behavior of a fluid phase, while those of HFSE concentrations are controlled by the chemistry of source and the crystal/melt process [31]. Pitcher [33,34], Barbarin [35] and Atherton and Tarney [36] classified the granitoid based on tectonic setting. N-MORB normalized multi-element patterns of granitoids in subduction zone show decoupled high LILE/HFSE signature while MORB-like trend and the other granitoids have a lesser LILE/HFSE offset and large Ba and Ti troughs reflecting an intraplate nature [37]. Nb anomalies relative to Th and Ce which are significant signatures of subduction-related zone [38]. Eu anomaly resulted from plagioclase [39].

All the felsic to intermediate rocks Group I, Group II, and Group III are compositionally ranging from rhyolite, monzogranite via quartz monzonite, to granodiorite with titanite and hornblende as a minor constituent, characteristic of I-type granitic rocks. In addition, the rocks are I-type on K_2O versus Na_2O (**Figure 6(a)**) [40] and total FeO versus CaO (**Figure 6(b)**) [41]. The existence of titanite and hornblende in Group II and Group III are agreement with the characteristic of I-type granitic rocks. Group I was form in the fields of volcanic arc and syn-collision environment while Group II and Group III rocks form a cluster in the fields of upper boundary for oceanic ridge granite from anomalous ridge on Nb versus Y diagram (**Figure 6(c)**) [42]. Sr versus Nb+ Y diagram (**Figure 6(d)**) [43] show Group I rocks are volcanic arc or post-collision granite and Group II and Group III rocks are within plate or post-collision granite. The REE patterns of rocks are parallel trend that are co-magmatic origin**.** REE patterns show slightly negative Eu anomalies (**Figure 5(a)**), resulted from plagioclase fractionation [39]. The N-MORB normalized multi-element patterns (**Figure 5(b)**) are LILE enrichment indicted the granitoids in subduction zone [37]. Group I and Group II not show negative Nb anomalies relative to Th and Ce which are not significant signatures of subduction-related magma while Group III show negative Nb anomalies relative to Th and Ce which are significant signatures of subduction-related magma [38].

The intermediate to mafic plutonic rocks, Group IV are monzonite- quartz monzonite-diorite-gabbroic diorite. Although the mineral composition is difference, geochemical character is similar**.** Tectonic discrimination diagrams for basic rocks that include the fields of calc-alkaline rocks and their possible environments of formation have been applied to Group VI rock. The rock appears to be island arc and continental margin on FeO - MgO - Al_2O_3 plot (**Figure 7(a)**) [44], calc-alkaline magma on Ti - Zr - Sr (**Figure 7(b)**) [45] and Ti - Zr - Y (**Figure 7(c)**) plots [45], and calc-alkaline and continental margin volcanic arc and polygenetic crust island arc on normalized Th - Nb plot (**Figures 7(d)** and **7(e)**) [46]. REE patterns show a negative Eu anomaly (**Figure 5(a)**), resulted from plagioclase fractionation [39]. N-MORB normalized multi-element patterns (**Figure 5(b)**) are LILE enrichment indicted the granitoids in subduction zone [37] and show negative Nb anomalies relative to Th and Ce which are significant signatures of subduction-related magma [38].

Thone Felsic rocks in Group II and Group III plutonic rock and Group I volcanic rock are dominant I-type, calc-alkaline, subduction-related titanite, hornblende and biotite granite magmatism. Felsic rocks are volcanic arc, within plate or post-collision granites. The intermediate to mafic plutonic rocks in Group IV are transition from low K calc-alkaline to shoshonitic rocks that is the feature of continental volcanic arc magma. Thone plutonic and volcanic rocks show the enrichment in LILE relative to HFSE that is standard subduction signatures in volcanic arc granites [37,38,43]. Based on petrography, geochemistry and field relationship (relate with volcanic and volcano-sedimentary rocks), Thoen plutons are assigned to be part of EGB of Southeast Asia that sporadically continues northward to Mae Chan plutons [13] and southward to Tak batholith [47], and Uthai Thani [48,49] and indicated the magmatism along the boundary between Sukhothai Arc and Inthanon Zone [17].

The amalgamation of the Sibumasu and the Indochina blocks in Thailand will be debated for identified location, boundary, and timing. The plutonic rocks in Thailand occurred related to syn- and post-collision between the Sibumasu and the Indochina blocks. The subduction of the Paleo-Tethys Ocean switch to the collision of the Sibumasu block and the Indochina block in the middle Triassic (237 Ma), the syn- collisional orogenic events in middle to late Triassic (230 - 237 Ma) and post-collisional orogenic events in late Triassic (200 - 230 Ma) [13]. The tectonic model for Thoen igneous rocks (**Figure 8**) was modified from Wang *et al.* [13] and Watthanapond *et al.* [48]. Early to middle Triassic, the Paleo-Tethys Ocean plate was east-subducted beneath the Sukhothai zone or Indochina block that was the occurring igneous rock in EGB and Group I, Group II, Group III and Group IV rocks of Thoen igneous rock. Age dating of granite of EGB in Mae Chan Chiang Rai is 226 ± 3 Ma [13], and Uthai Thani is 222 Ma [48]. Late Triassic period, the hybridized magma was generated and emplacement to be is muscovite-biotite-granite with 194 - 209 Ma in age [48].

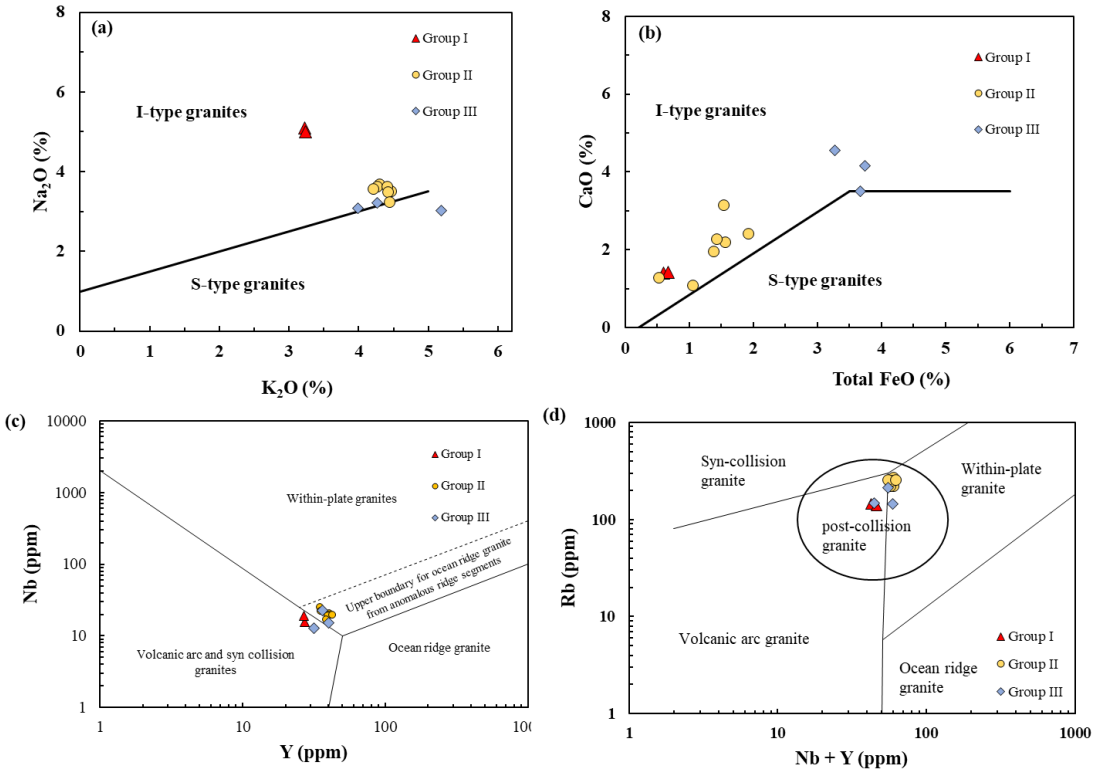

Figure 6 Positions of the studied, Group I rhyolite, Group II granite, and group III quartz monzonite, monzonite, diorite, and granodiorite in (a) Na_2O versus K_2O [40], (b) CaO versus FeO(total) [41], (c) Nb versus Y [42], and (d) Rb versus Nb + Y [43] diagrams.

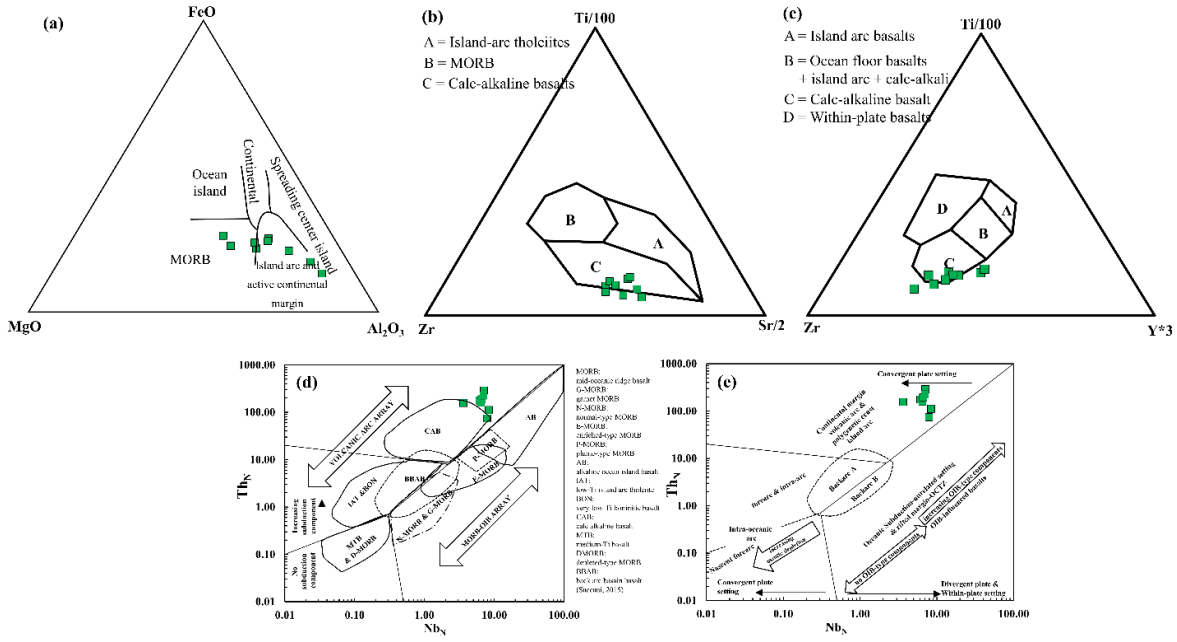

Figure 7 Positions of the studied, Group IV rocks in (a) FeO - MgO - Al_2O_3, [44] (b) Ti - Zr - Sr [45] and (c) Ti - Zr - Y [45], and (d,e) chondrite-normalized Th - Nb diagrams [46].

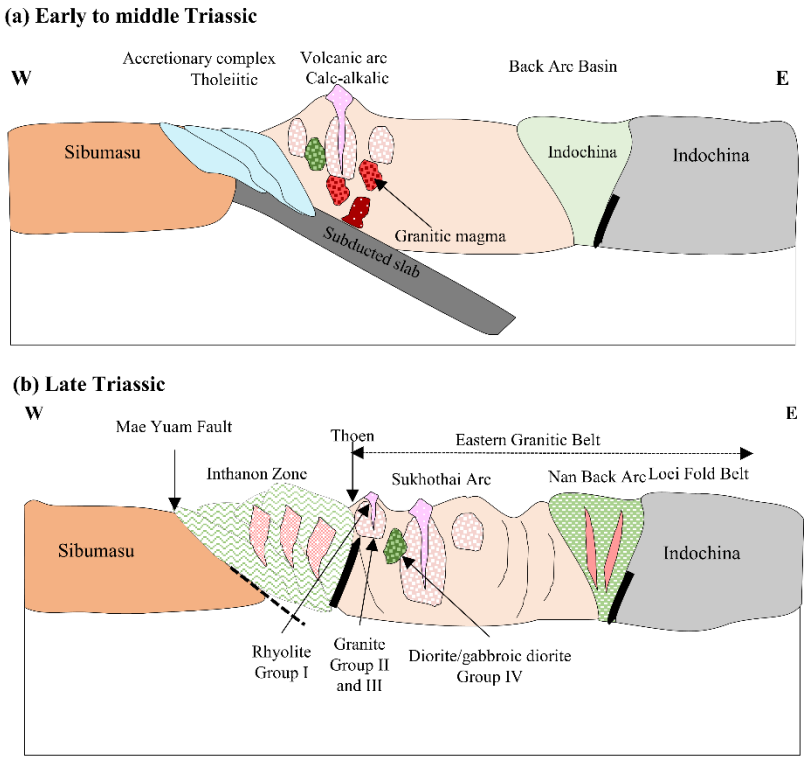

Figure 8 Tectonic model of the magmatism in EGB, Thailand (Modified after Wang *et al.* [13] and Watthanapond *et al.* [48]).

Conclusions

The plutonic rocks in the area of Lom Rat sub-district, Thoen District, Lampang Province are dominantly felsic, intermediate to mafic plutonic rocks and minor felsic volcanic rocks. The petrography and geochemistry can be used to classify the igneous rock samples and summarized as follows:

Thoen plutonic rock samples composed of Group I volcanic rock, Group II felsic plutonic rock, Group III intermediate plutonic rock, Group IV intermediate to mafic rocks.

Major and trace elements data from Thoen felsic to intermediate plutonic rocks and felsic volcanic rock are the presence of mainly high-K calc-alkaline granite, indicated the magmatic affinity as calc-alkaline with I-type magma series that an active continental margin, with the involvement of continental crust. The intermediate to mafic plutonic rocks are ranging from low K to high-K calc-alkaline and shoshonitic series, indicated the feature of continental volcanic arc magma.

Chondrite-normalized REE patterns of Thoen plutonic rocks are variable enrichments in LREE, and depletions in HREE that typical of I-type volcanic arc granites.

N-MORB normalized multi-element patterns of Thoen plutonic rocks are variable LILE enrichments in Rb, Ba, Th and Ce, and depletions in Ta, Nb, Sr and Ti, that are typical of I-type volcanic arc granites.

Thoen pluton is the part of EGB and can be correlated with the Tak pluton, and the pluton in East Malaya province, Malaysia and was indicated the magmatism along the boundary between Sukhothai Arc and Inthanon Zone.

Acknowledgements

The authors would like to acknowledge financial support from the Faculty of Science, Chiang Mai University; Department of Geological Sciences, Faculty of Science, Chiang Mai University; Department of Mineral Resources; and Geoscience program, Mahidol University, Kanchanaburi campus, Thailand.

Declaration of Generative AI in Scientific Writing

The authors acknowledge the use of generative AI tools (Grammarly and ChatGPT) in the preparation of this manuscript, specifically for language editing and grammar correction. No content generation or data interpretation was performed by AI. The authors take full responsibility for the content and conclusions of this work.

CRediT Author Statement

Patcharin Kosuwan Jundee: Conceptualization, Methodology, Investigation, Supervision, Validation, Visualization, Funding acquisition, and Writing original draft, review & editing.

Burapha Phajuy: Supervision, and Validation.

Phisit Limtrakun: Supervision, and Validation.

Apichet Boonsoong: Supervision, and Validation.

Panjai Saraphanchotwitthaya: Funding acquisition and Writing original draft.

Ekkachak Chandon: Formal analysis, Data curation and Funding acquisition.

Thanittha Suatrong: Methodology, Formal analysis, Investigation, and Data curation.

Pinpan Thapthanee: Methodology, Formal analysis, Investigation, and Data curation.

References

[1] EJ Cobbing, DIJ Mallick, PEJ Pitfield and LH Teoh. The granites of the Southeast Asian Tin Belt. *Journal of the Geological Society London* 1986; **143(3)**, 537-550.

[2] P Charusiri, AH Clark, E Farrar, D Archibald and B Charusiri. Granite belts in Thailand: Evidence from the $^{40}Ar/^{39}$ Ar geochronological and geological syntheses. *Journal of Southeast Asian Earth Science*s 1993; **8(1-4)**, 127-136.

[3] RL Linnen. Depth of emplacement, fluid provenance and metallogeny in granitic terranes: A comparison of western Thailand with other tin belts. *Mineralium Deposita* 1998; **33(5)**, 461-476.

[4] P Putthapiban. Geology and geochronology of igneous rocks of Thailand. *In:* Proceedings of the Symposium on Geology of Thailand, Department of Mineral Resources, Bangkok, Thailand. 2002, p. 261-283.

[5] P Charusiri, T Pungrassami and G Sinclair. Classification of rare-earth element (REE) deposit in Thailand: A genetic model. *Journal of the Geological Society Thailand* 2006; **1(1)**, 57-66.

[6] K Phountong, A Salam and T Manaka. Petrochemistry of granite from Takua Pit Thong area, Ratchaburi, Thailand. *Bulletin of Earth Science of Thailand* 2020; **12(1)**, 15-29.

[7] MP Searle, MJ Whitehouse, L Robb, AA Ghani, CS Hutchison, M Sone, SWP Ng, MH Roselee, SL Chung and JGH Oliver. Tectonic evolution of the Sibumasu-Indochina terrane collision zone in Thailand and Malaysia: Constraints from new U-Pb zircon chronology of SE Asian tin granitoids. *Journal of the Geological Society* 2012; **169(4)**, 489-500.

[8] PK Jundee, S Phanbuppha, T Jamsai and B Phajuy. Petrochemistry of granitic rock in Tha Pai area, Mae Hi Sub-District, Pai District, Mae Hong Son Province, Thailand. *Songklanakarin Journal of Science and Technology* 2022; **44(6)**, 1427-1433.

[9] PK Jundee, S Chaiwchan, S Inthacharoensarn, B Phajuy and P Nontarak. Petrochemistry and tectonic setting of the Phroa-Wiang Pa Pao Granitic Rocks, Chiang Mai, and Chiang Rai Provinces, Central Granitic Belt of Thailand. *Trends in Sciences* 2024; **21(10)**, 8055.

[10] CK Morley. A tectonic model for the Tertiary evolution of strike-slip faults and rift basins in SE Asia. *Tectonophysics* 2002; **347(4)**, 189-215.

[11] AA Ghani, MP Searle, L Robb and SL Chung. Transitional I S type characteristic in the Main Range granite, peninsular Malaysia. *Journal of Asian Earth Sciences* 2013; **76**, 225-240.

[12] AA Ghani, CH Lo and SL Chung. Basaltic dykes of the Eastern Belt of Peninsular Malaysia: the effects of the difference in crustal thickness of Sibumasu and Indochina. *Journal of Asian Earth Sciences* 2013; **77**, 127-139.

[13] Y Wang, H He, P Cawood, W Fan, B Srithai, Q Feng, Y Zhang and Q Xin. Geochronology, elemental and Sr-Nd-Hf-O isotopic constraints on the petrogenesis of the Triassic post-collisional granitic rocks in NW Thailand and its Paleotethyan implications. *Lithos* 2016; **266(3-4)**, 264-286.

[14] Q Xin, Q Feng, Y Wang, T Zhao, JW Zi, M Udchachon and Y Wang. Late Triassic post-

collisional granites related to Paleotethyan evolution in SE Thailand: Geochronological and geochemical constraints. *Lithos* 2017; **286**, 440-453.

[15] P Nualkhao, R Takahashi, A Imai and P Charusiri. Petrochemistry of granitoids along the Loei Fold Belt, Northeastern Thailand. *Resource Geology* 2018; **68(4)**, 1-30.

[16] A Fanka and S Nakapadungrat. Preliminary study on petrography and geochemistry of granitic rocks in the Khao Phra - Khao Sung area, Amphoe Nong Bua, Changwat Nakhon Sawan, Central Thailand. *Bulletin of Earth Science of Thailand* 2018; **10(1)**, 55-68.

[17] X Qian, Y Wang, Y Zhang, Y Wang and V Senebouttalath. Late Triassic post-collisional granites related to Paleotethyan evolution in northwestern Lao PDR: Geochronological and geochemical evidence. *Gondwana Research* 2020; **84**, 163-176.

[18] E Uchida, S Nagano, S Niki, K Yonezu, Y Saitoh, KC Shin and T Hirat. Geochemical and radiogenic isotopic signatures of granitic rocks in Chanthaburi and Chachoengsao provinces, southeastern Thailand: Implications for origin and evolution. *Journal of Asian Earth Science X* 2022; **8,** 100111.

[19] S Piyasin. *Geological Map of Thailand NE47-11. 1:250,000 (Changwat Uttaradit)*. Department of Minerals and Resources, Bangkok, Thailand. 1974.

[20] Department of Minerals and Resources. *Geological map of Lampang province*. Department of Minerals and Resources, Bangkok, Thailand. 2007.

[21] CS Hutchison. *Laboratory handbook of petrographic techniques*. John Wiley and Sons, Inc., New York, USA. 1973, p. 527.

[22] K Govindaraju and I Roelandts. Second report (1993) on the first three GIT-IWG rock reference samples: Anorthosite from Greenland, AN-G; basalt D' Essey-la-Côte, BE-N; granite De Beauvoir, MA-N. *Geostandards and Geoanalytical Research* 1993; **17(2)**, 227-294.

[23] N Imai, S Terashima, S Itoh and A Ando. 1994 complication of analytical data for minor and trace elements in seventeen GSJ geochemical reference samples, "Igneous rock series". *Geostandards and Geoanalytical Research* 1995; **19(2)**, 135-213.

[24] A Streckeisen. To each plutonic rock its proper name. *Earth-Science Reviews* 1976; **12(1)**, 1-33.

[25] RR Large, JB Gemmell, H Paulick and DL Huston. The alteration box plot: a simple approach to understanding the relationship between alteration mineralogy and lithogeochemistry associated with volcanic-hosted massive sulfide deposits. *Economic Geology* 2001; **96(5)**, 957-971.

[26] EAK Middlemost. Naming materials in the magma/igneous rock system. *Earth-Science Reviews* 1994; **37(3-4)**, 215-224.

[27] TNJ Irvine and WRA Baragar. A guide to the chemical classification of the common volcanic rocks. *Canadian Journal of Earth Sciences* 1971; **8(5)**, 523-548.

[28] JA Winchester and PA Floyd. Geochemical discrimination of different magma series and their differentiation products using immobile elements. *Chemical Geology* 1977; **20**, 325-343.

[29] PC Rickwood. Boundary lines within petrologic diagrams which use oxides of major and minor elements. *Lithos* 1989; **22(4)**, 247-263.

[30] SR Taylor and MK Gorton. Geochemical application of spark source mass spectrography—III. Element sensitivity, precision and accuracy. *Geochimica et Cosmochimica Acta* 1977; **41(9)**, 1375-1380.

[31] HR Rollinson. *Using geochemical data: Evaluation, presentation, interpretation*. Longman Scientific & Technical. Harlow, England, 1993, p. 380.

[32] SS Sun and WF McDonough. Chemical and isotopic systematics of oceanic basalt: Implications for mantle composition and processes. *Geological Society, London, Special Publications* 1989; **42(1)**, 313-345.

[33] WS Pitcher. *Granite type and tectonic environment*. *In:* K Hsu (Ed.). Mountain building processes. Academic Press, London, England, 1983, p. 19-40.

[34] WS Pitcher. *The nature and origin of granite*. Blackie, London, 1993, p. 321.

[35] B Barbarin. Granitoids: Main petrogenetic classification in relation to origin and tectonic setting. *Geology Journal* 1990; **25(3-4)**, 227-238.

[36] MP Atherton and J Tarney. *Origin of granite batholiths: Geochemical evidence*. Shiva Publishing Limited, Orpington, England, 1979, p. 148.

[37] JD Winter. *Principles of igneous and metamorphic petrology*. Pearson New International Edition. Pearson Education Limited, Harlow, England, 2014, p. 745.

[38] J Baier, A Audétat and H Kepple. The origin of the negative niobium tantalum anomaly in subduction zone magmas. *Earth and Planetary Science Letters* 2008; **267(1-2)**, 290-300.

[39] AD Fowler and R Doig. The significance of europium anomalies in the REE spectra of granites and pegmatites, Mont Laurier, Quebec. *Geochimica et Cosmochimica Acta* 1983; **47(6)**, 1131-1137.

[40] BW Chappell and AJR White. Two contrasting granite types. *Pacific Geology* 1974; **8**, 173-174.

[41] BW Chappell and AJR White. Two contrasting granite types: 25 years later. *Australian Journal of Earth Sciences* 2001; **48(4)**, 489-499.

[42] JA Pearce, NBW Harris and AG Tindle. Trace element discrimination diagrams for the tectonic interpretation of granite rocks. *Journal of Petrology* 1984; **25(4)**, 956-983.

[43] J Pearce. Sources and settings of granitic rocks. *Episodes* 1996; **19(4)**, 120-125.

[44] TH Pearce, BE Gorman and TC Birkett. The relationship between major element chemistry and tectonic environment of basic and intermediate volcanic rocks. *Earth and Planetary Science Letters* 1977; **36(1)**, 121-132.

[45] JA Pearce and JR Cann. Tectonic setting of basic volcanic rocks determined using trace element analyses. *Earth and Planetary Science Letters* 1973; **19(2)**, 290-300.

[46] E Saccani. A new method of discriminating different types of post-Achean ophiolite basalts and their tectonic significance using Th-Nb and Ce-Dy-Yb systematics. *Geoscience Frontiers* 2015; **6(4)**, 4158-501.

[47] B Phajuy and V Singtuen. Petrochemical characteristics of Tak volcanic rocks, Thailand: Implication for tectonic significance. *ScienceAsia* 2019; **45(4)**, 350-360.

[48] P Watthanapond, A Fanka, K Pang and S Chung. Petrogenesis of REE-mineralized granitic plutons in central Thailand, Southeast Asian tin belt: New insights from geochemistry and zircon U-Pb geochronology. *Journal of Asian Earth Sciences* 2025; **277**, 106368.

[49] PK Jundee, P Limtrakun, A Boonsoong and Y Panjasawatwong. Petrography and REE geochemical characteristics of felsic to mafic volcanic/hypabyssal rock in Nakhon Sawan and Uthai Thani Provinces, Central Thailand. *Chiang Mai Journal of Science* 2017; **44(4)**, 1722-1734.